Space Sci Rev
DOI 10.1007/s11214-011-9768-x

# A Comparison of Ground Level Event e/p and Fe/O Ratios with Associated Solar Flare and CME Characteristics

**S.W. Kahler · E.W. Cliver · A.J. Tylka · W.F. Dietrich**

Received: 17 June 2010 / Accepted: 3 March 2011
© U.S. Government 2011

**Abstract** Solar energetic particle (SEP) events reaching rigidities >1 GV are observed at 1 AU as ground-level events (GLEs). They are considered to be extreme cases of gradual SEP events, produced by shocks driven by wide and fast CMEs that are usually associated with long-duration (>1 hour) soft X-ray (SXR) flares. However, some large gradual SEP events, including GLEs, are associated with flares of short-duration (<1 hour) timescales comparable to those of flares seen with impulsive, low-energy SEP events with enhanced charge states, heavy-element abundances, and e/p ratios. The association of some GLEs with short-duration SXR events challenges us to understand the GLE event-to-event variation with SXR durations and whether it truly reflects the nature of the particle acceleration processes or simply the characteristics of the solar regions from which large, fast CMEs arise. We examine statistically the associated flare, active region (AR), and CME characteristics of ∼40 GLEs observed since 1976 to determine how the GLE e/p and Fe/O ratios, each measured in two energy ranges, depend on those characteristics. The abundance ratios trend weakly to lower, more coronal, and less scattered values with increasing flare timescales, thermal and nonthermal peak fluxes, and measures of source AR sizes. These results and the wide range of solar longitude connections for GLEs with high abundance ratios argue against a significant role for flare effects in the GLEs. We suggest that GLE SEPs are accelerated predominately in CME-driven shocks and that a coupling of flare size and timescales with CME properties could explain the SEP abundance correlations with flare properties.

S.W. Kahler (✉) · E.W. Cliver
Air Force Research Laboratory, RVBXS, 29 Randolph Rd., Hanscom AFB, MA 01731-3010, USA
e-mail: stephen.kahler@hanscom.af.mil

E.W. Cliver
e-mail: afrl.rvb.pa@hanscom.af.mil

A.J. Tylka
Space Science Division, Naval Research Laboratory, Code 7671, Washington, DC 20375, USA

W.F. Dietrich
Praxis, Inc., Alexandria, VA 22303, USA

Published online: 15 April 2011

**Keywords** Acceleration of particles · Interplanetary medium · Sun: particle emission · Sun: radio radiation · Sun: coronal mass ejections

## 1 Introduction

### 1.1 The Two-Class SEP System

Two distinct classes of solar energetic particle (SEP) events at 1 AU, impulsive and gradual, have long been recognized (Reames 1995, 1999; Klecker et al. 2007; Cliver 2009b). Impulsive SEP events are characterized by particle durations of hours at ∼1 MeV/nuc, relatively high ratios of electrons to protons (e/p), $^3$He/$^4$He, Fe/O, high ionic charge states (Klecker et al. 2006) and strong enhancements of elements of Z ≥ 34 (Reames 2000; Reames and Ng 2004; Mason et al. 2004; Leske et al. 2007), in addition to their associations with short-duration solar H$\alpha$ and SXR flares, strong type III bursts, narrow or no coronal mass ejections (CMEs) (Kahler et al. 2001; Yashiro et al. 2004) and narrow solar-longitudinal ranges of propagation (Reames 1999). The energy range of impulsive SEPs is usually ≤ 10 MeV/nuc, and the particles are thought to escape along open field lines (Reames 2002) from magnetically well connected flares. Gradual SEP events are characterized by large fluences, durations of days, near-coronal elemental abundances and charge states, at least at ∼MeV/nucleon energies, and particle energies extending occasionally to the GeV range, thereby becoming GLEs. Their close association with metric and decametric/hectometric type II bursts (Cliver et al. 2004) and with wide ($W > 60°$) and fast ($v >$ 900 km/s) CMEs (Gopalswamy et al. 2008) indicates acceleration at CME-driven shocks.

An observational connection between classes of flares and classes of SEP events (Cane et al. 1986, hereafter CMvR) was motivated by the identification of a class of interplanetary SEP events with high ratios of $E > 4$ MeV relativistic electron fluxes to $E > 10$ MeV proton fluxes (e/p). The association of electron-rich events with impulsive flares led CMvR to associate the high e/p SEP events with the compact, short-duration SXR flares and low e/p SEP events with large, long-duration flares high in the solar corona. When this picture was challenged by a survey of large SEP events through 2005 showing a broad range of event Fe/O values at $E > 25$ MeV/nuc, Cane et al. (2006) took the Fe/O ratios as the basis for defining two classes of SEP events: one with rapid onsets and Fe-rich abundances originating directly in flares and the other with intensity peaks at the times of IP shock passage and Fe-poor abundances produced in shock acceleration. However, the lack of bimodal distributions of SEP events based on Fe/O ratios at $E > 25$ MeV led Cane et al. (2008) to suggest that large SEP events are comprised of contributions from both flares and shocks. They further suggested that elemental abundances at higher (>10 MeV/nuc) energies could not be compared with those determined at lower (2–10 MeV/nuc) energies to test for flare particles, a view advanced earlier by Reames and Ng (2004). The finding in large gradual SEP events at $E \geq 10$ MeV/nuc of the high ionic charge states (Mazur et al. 1999; Klecker et al. 2007) characteristic of impulsive SEPs added new complexity to the presumed two-class structure of SEP events.

As reviewed by Klecker et al. (2007) and Cliver (2009a), two prominent approaches have addressed the high-energy abundance enhancements. The first, by Cane et al. (2002, 2003, 2006), argues that the flare process directly produces the impulsive SEPs up to the observed high energies and that the shock is producing lower energy particles with the typical gradual SEP characteristics. A second approach by Tylka et al. (2005, 2006) is that the enhanced

heavy element abundances are the result of predominantly quasi-perpendicular shock acceleration which requires the higher seed particle threshold energies of remnant flare particles in the corona (Tylka and Lee 2006).

If the concept of extending the established low-energy ($E \leq 10$ MeV/nuc) impulsive SEP acceleration mechanism to much higher energies is valid, then evidence of impulsive SEPs from flares should be found in the most energetic SEP events, which have relatively short timescales and are likely to be produced by a single dominant acceleration mechanism. We explore the question of direct flare contributions to high-energy SEP events (Cane et al. 2006, 2008) by selecting for analysis the ground-level events (GLEs) observed since 1973. Their high threshold energies ($E \geq 430$ MeV/nuc) and usually intense emissions from associated flares provide the optimum set of SEP events for a test of the presence of impulsive SEPs.

### 1.2 The SEP Two-Class System and GLEs

The GLE observations have been interpreted with two opposing scenarios. In the first there are two separate injection components, one prompt and one delayed (e.g., Masson et al. 2009). The prompt component is produced in the associated flare at the beginning of its eruptive phase and observed at 1 AU with an impulsive rise, a hard energy spectrum, and a high anisotropy (Perez-Peraza et al. 2009). The delayed component is produced in the subsequent CME-driven shock (e.g., McCracken et al. 2008) or in expanding magnetic loops by stochastic acceleration (Perez-Peraza et al. 2009; Miroshnichenko et al. 2009) and is characterized by softer energy spectra and less anisotropy. Among the two-component advocates there is disagreement about the frequency of one versus two components. Vashenyuk et al. (2009) found two components in all 32 GLEs they examined, McCracken et al. (2008) in 13 of 15 magnetically well connected GLEs, but Moraal et al. (2009) in only 3 to 6 of the 16 GLEs of their study. Frequent complications in all of these studies, which interpret structure in the neutron monitor timelines, are changing directions of interplanetary magnetic fields and the limited field of view of any neutron monitor station. These factors can conspire to produce artificial peaks in the neutron-monitor intensity-time profiles which have nothing to do with different particle acceleration processes at the Sun. In addition, the notion that differences in particle angular distributions from flare and shock accelerations at the Sun are preserved in the observed angular distributions at 1 AU is highly questionable.

The other observational scenario considers only a single dominant GLE component, which is produced in CME-driven shocks. Reames (2009a, 2009b) found by detailed fits of SEP onset times for 30 GLEs that the SEP release times followed the onsets of shock-induced type II radio bursts and that the associated CME heights increased with increasing longitudinal displacements of the solar source regions, as expected for shocks. Temporal variations in the GLE intensity and anisotropy profiles would be due to interplanetary conditions (Saiz et al. 2005) or variations in the shock source conditions. Gopalswamy et al. (2005a) also found that type II bursts preceded the release of particles in GLEs, supporting the shock acceleration model. He suggested that particles from major accompanying flares should also be present in GLEs, observable at 1 AU only for well connected flares, but he did not specify how those particles might be observed.

Before the discovery in the 1970s of CMEs as important solar energetic events, the good correlations between peak SEP event intensities and associated solar flare emission signatures were taken as clear evidence of solar flares as the only source of gradual SEP events. Subsequent work has shown a dominant role of CME-driven shocks for gradual SEP events, but SEP intensities often correlate little better with CME characteristics such as speed $v$ or width $W$ than with SXR flare sizes (Gopalswamy et al.

2003, 2004; Cane et al. 2008). In a given CME speed range the associated SEP intensities can vary up to four orders of magnitude (Kahler 2001), clearly indicating the importance of factors other than CME speeds in SEP production. The high associations of SEP events with metric and decametric-hectometric type II radio bursts (Cliver et al. 2004), the importance of preceding interplanetary SEP backgrounds (Kahler 2001; Cliver 2006), and the lack of a difference in the flare signature of integrated 1 MHz type III emission between impulsive and gradual SEP events (Cliver and Ling 2009) are examples of evidence supporting shocks as sources of gradual SEP events. The focus of this study is whether the flare-site processes, instead of the CME-driven shock, is the dominant particle-production mechanism in some GLEs, particularly at ion energies above a few tens of MeV/nucleon or electrons above ∼1 MeV.

The interpretation of one or two GLE injection components has thus far been based only on the early time profiles of the GLE intensities at 1 AU and assumed little if any coupling between the two particle populations. Since studies based on SEP compositions, rather than SEP intensities, have been useful in past work in establishing the two basic kinds of SEP events, we will take the SEP compositions, or, more exactly, SEP abundance ratios, as our analytical tool in this study. We can look for evidence of a flare dependence for GLE abundance parameters (e/p or Fe/O ratios) separately at high or low energies, depending on the nature of the composition of the flare particles and whether they are directly injected or provide energetic seed particles for the accompanying CME-driven shock (e.g., Tylka et al. 2005; Tylka and Lee 2006; Desai et al. 2007).

Finding a connection of the elemental abundance characteristics of GLEs with properties of associated flares or active regions could not only support a two-component model but provide some insights into the spatial, energetic, and perhaps temporal nature of the coupling. Examples of the enhanced ion temperatures and elemental abundance effects found in gradual SEP events (Cane and Lario 2006; Klecker et al. 2007) have also been found in post-CME current sheets (Ciaravella et al. 2002; Ko et al. 2003), but attempts to relate the two energetic particle populations have been limited to simple schematics (Kocharov and Torsti 2002; Cliver et al. 2004) rather than detailed physical models.

One clue about the origin of SEP species in large events may come from comparisons of abundance enhancements with total flare sizes or SEP fluences. In impulsive SEP events Reames et al. (1988) found declining $^3$He/$^4$He ratios with increasing measures of flare intensities and suggested that a saturation effect was occurring in small flare source regions. The alternative interpretation that dilution by additional shock acceleration of coronal material caused the declining $^3$He/$^4$He ratios could be ruled out by a lack of a similar effect with Fe/O ratios in the impulsive SEP events and by a lack of a correlation between $^3$He/$^4$He and Fe/O ratios (Reames 1990; Reames et al. 1994).

In the context of the CMvR two-class SEP structure, Kahler et al. (1991) had found four GLEs associated with short-duration (defined as $<$1 hour duration) SXR flares, suggesting SEP production in the flare impulsive phase as a possible alternative to second-phase shock acceleration. Since 1991 we have observed 20 more GLEs, 7 associated with short-duration SXR flares, and measured their e/p and elemental abundances, so we can now carry out a broader comparison of GLE properties with several associated flare and CME characteristics. Studies of variability and systematic trends in Fe/O in large SEP events are generally complicated by the fact that SEP Fe/O not only varies from event to event, but also with energy in a given event. Using Fe/O measurements at 30–40 MeV/nucleon and associated SXR durations for large SEP events in 1997–2005, Cliver (2009b) found a tendency of declining ratios with increasing flare durations. The question is whether in the GLEs, the most energetic of SEP events, the e/p and Fe/O ratios are ordered in any way by the flare and/or

CME characteristics. The 2 to 100 keV electrons are strongly tied to the flare impulsive phase through their associations with $^3$He/$^4$He enhancements and type III bursts (Reames et al. 1988), but it is particularly unclear and contentious whether the $E > 20$ MeV/nuc heavier elements observed in space are also accelerated in flares or in shocks or both, or which process is dominant.

The GLEs are the most energetic events we observe, so they should present the most stringent challenge to the flare acceleration scenario. The characteristics of flares associated with pure impulsive interplanetary SEP events with low ($E \leq 10$ MeV/nuc) energies (Reames 1999) or with high e/p ratios (CMvR) were described in Sect. 1. To carry out statistical tests for evidence of significant flare acceleration in GLEs, we have to make assumptions about the characteristics of those associated flares, which are generally larger than those encountered in the earlier studies with SEP events of lower energies. Following those studies, we assume that flare-SEP contributions are more likely from flares with shorter timescales, smaller spatial source regions, more intense impulsive or thermal phases, and better magnetic connection to Earth. The corresponding SEP signatures are assumed to be enhanced e/p and Fe/O ratios. The opposite trends in flare properties are expected if the CME characteristics become more important when shock-accelerated SEPs are dominant. We parameterize these contributions in the following data analysis.

## 2 Data Analysis

### 2.1 The GLE Particle Data

We characterize each of GLEs #26–70 with four energetic particle abundance parameters, two e/p fluence ratios and two Fe/O fluence ratios, where each ratio is an event-averaged value. For each ratio pair we chose two energy ranges differing by more than an order of magnitude to attempt to find flare effects or contributions to the GLEs which might be evident only in particular energy ranges. Our analytic approach is to compare the particle abundance parameters statistically with various flare, active region (AR), and CME parameters given in Table 1 for GLEs #26–54 and Table 2 for GLEs #55–70 to determine which particle species and energies might be organized by the solar event values. We rely on the occurrence of significant correlations in a sample of up to 45 GLEs as a guide to isolate the important relationships. For events prior to 1986, we obtained $E > 30$ MeV proton fluences from IMP8; after 1986, these fluences were provided by the Space Environment Monitor data from various GOES satellites and available at the National Geophysical Data Center web site.

The $E > 430$ MeV event fluences for each GLE were obtained from an analysis of neutron monitor data (Tylka and Dietrich 2009), cross-checked with satellite measurements from IMP8, SAMPEX, and GOES at comparable energies whenever possible. The error bars of the >430 MeV proton fluences are ∼5 to 15% of the fluences. The $E > 1$ MeV electron fluences were obtained from the University of Chicago's Cosmic Ray Nuclei Experiment (CRNE) on IMP8, using a recent simulation of the instrument's acceptance for electrons (Novikova et al. 2010). We assigned nominal error bars of 10% and 5% to the >1 MeV electron and >30 MeV proton fluences, respectively. The event ratios of the $E > 1$ MeV electron fluences to the $E > 30$ MeV proton fluences (hereafter e/p low) and to the $E > 430$ MeV proton fluences (hereafter e/p high) are given in the third and fourth columns of Tables 1 and 2.

For the low-energy Fe/O ratios of GLEs #27–54 we used fluences at 4–6 MeV/nuc from the Very Low Energy Telescope on the IMP-8 spacecraft. No ratios were available for GLEs

**Table 1** GLE SEP Fluence Ratios and Flare, AR and CME Properties

| GLE No. | Date yymmdd | e/p low[a] | e/p high[b] | Fe/O low[c] | Fe/O high[d] | Longitude and peak | Flare dura[e] | Flare rise[e] | Spot area[f] | No. ARs | CME width[g] |
|---|---|---|---|---|---|---|---|---|---|---|---|
| 26 | 730429 | 5.11 | 1118.3 | NA | NA | W73 X1 | 93 | 5 | 500 | 0 | NA |
| 27 | 760430 | 1.41 | 716.4 | 6.40 ± 1.78 | 9.0 5.4/3.6 | W47 X2 | 62 | 14 | 200 | 1 | NA |
| 28 | 770919 | 1.00 | 578.4 | 1.70 ± 0.17 | 11.0 2.2/2.2 | W58 X2 | 89 | 21 | 800 | 1 | NA |
| 29 | 770924 | 2.06 | 253.1 | 4.48 ± 0.63 | 9.2 1.0/1.0 | W120 NA | NA | NA | 800 | 1 | NA |
| 30 | 771122 | 1.57 | 256.9 | 0.97 ± 0.14 | 6.7 1.5/1.5 | W40 X1 | 63 | 6 | 200 | 2 | NA |
| 31 | 780507 | 1.91 | 484.3 | 6.51 ± 1.53 | 4.9 3.3/2.1 | W72 X2 | 79 | 7 | 900 | 1 | NA |
| 32 | 780923 | 0.25 | 586.2 | 1.03 ± 0.09 | 8.9 2.9/2.3 | W50 X1 | 189 | 32 | 600 | 2 | NA |
| 33 | 790821 | NA | NA | NA | NA | W40 C6 | NA | NA | 0 | 3 | 110 |
| 34 | 810410 | 1.03 | NA | 3.73 ± 1.11 | 10.0 13/6 | W36 X2 | 52 | 9 | 200 | 4 | 45 |
| 35 | 810510 | NA | NA | 0.56 ± 0.12 | 8.0 19/7 | W75 M1 | NA | NA | 300 | 4 | 80 |
| 36 | 811012 | 0.81 | 471.0 | 1.13 ± 0.12 | 1.7 0.5/0.5 | E31 X3 | 107 | 9 | 1300 | 4 | 360 |
| 37 | 821126 | 1.29 | 461.3 | 0.51 ± 0.12 | 6.2 6.0/3.3 | W87 X5 | 184 | 21 | 1500 | 0 | 60 |
| 38 | 821207 | 0.14 | 84.2 | 1.62 ± 0.17 | 5.4 1.9/1.5 | W86 X3 | 93 | 13 | 600 | 1 | 100 |
| 39 | 840216 | 0.31 | 60.6 | 6.09 ± 1.47 | 6.3 3.4/2.3 | W120 NA | NA | NA | 300 | 0 | 60 |
| 40 | 890725 | NA | NA | 0.00 ± 1.87 | 22.0 110/16 | W85 X3 | 18 | 4 | 200 | 0 | NA |
| 41 | 890815 | 0.16 | 148.9 | 1.07 ± 0.07 | 4.1 0.9/0.9 | W85 X20 | 94 | 19 | 800 | 2 | 55 |
| 42 | 890929 | 0.66 | 327.2 | 2.30 ± 0.13 | 0.9 0.1/0.1 | W105 X10 | 82 | 9 | 1200 | 0 | 77 |
| 43 | 891019 | 0.53 | 108.8 | 0.57 ± 0.08 | 3.8 0.3/0.3 | E09 X13 | 129 | 13 | 1000 | 2 | NA |
| 44 | 891022 | 0.22 | 331.1 | 1.62 ± 0.14 | 0.6 0.2/0.2 | W32 X3 | 105 | 20 | 900 | 3 | NA |
| 45 | 891024 | 0.25 | 37.1 | 1.22 ± 0.07 | 3.3 0.3/0.3 | W57 X6 | 197 | 48 | 900 | 3 | 108 |
| 46 | 891115 | 2.15 | 281.1 | 4.48 ± 1.89 | 5.0 3.4/2.4 | W28 X3 | 42 | 4 | 500 | 0 | 50 |
| 47 | 900521 | 1.45 | 681.9 | 3.89 ± 0.96 | 15.5 3.5/3.5 | W37 X5 | 23 | 5 | 600 | 0 | NA |
| 48 | 900524 | 1.49 | 235.7 | 2.60 ± 0.65 | 8.9 2.0/2.0 | W76 X9 | 18 | 2 | 400 | 0 | NA |
| 49 | 900526 | 2.63 | 286.6 | 2.72 ± 1.58 | 8.2 4.9/3.2 | W110 X1.4 | 37 | 8 | 400 | 0 | NA |
| 50 | 900528 | NA | NA | NA | 24.0 18/10 | W120 C1 | NA | NA | 400 | 0 | NA |
| 51 | 910611 | NA | NA | NA | NA | W15 X12 | 54 | 8 | 2200 | 0 | NA |
| 52 | 910615 | 0.33 | 216.4 | 0.90 ± 0.10 | 0.4 0.9/0.3 | W70 X1.2 | 88 | 6 | 2000 | 0 | NA |
| 53 | 920625 | 0.70 | 637.1 | 1.37 ± 0.13 | 2.5 0.6/0.6 | W69 X4 | 121 | 13 | 1100 | 1 | NA |
| 54 | 921102 | NA | NA | 1.66 ± 0.17 | NA | W90 X9 | 110 | 18 | 700 | 0 | NA |

[a]e/p low: (e > 1 MeV)/(p > 30 MeV)

[b]e/p high: (e > 1 MeV)/(p > 430 MeV)

[c]Fe/O low: Fe/O at 4–6 MeV/nuc from the IMP-8/VLET, normalized to average SEP value of 0.134

[d]Fe/O high: Fe/O at 47–80 MeV/nuc from IMP-8/CRNE, normalized to average SEP value of 0.134. Fe/O values are taken from Table 2 of Tylka et al. (2005) with additional values specifically for this energy range for events #36 and #42–45. Error bars (±) accompany each entry

[e]Duration above 10% of SXR peak in minutes; rise times from 10% of SXR peak to peak time in minutes

[f]Approximate areas of AR sunspots in millionths of a solar hemisphere

[g]Widths in degrees. CMEs for GLEs #33–42 from Solwind and SMM catalogs; CMEs for GLEs # 55–70 from Lasco SEEDS catalog

**Table 2** GLE SEP Fluence Ratios and Flare, AR and CME Properties *continued*

| GLE No. | Date yymmdd | e/p low[a] | e/p high[b] | Fe/O low[c] | Fe/O high[d] | Longitude and peak | Flare dura[e] | Flare rise[e] | Spot area[f] | No. ARs | CME width[g] |
|---|---|---|---|---|---|---|---|---|---|---|---|
| 55 | 971106 | 0.91 | 413.3 | 3.15 ± 0.02 | 5.81 ± 0.14 | W63 X9 | 21 | 7 | 800 | 0 | 113 |
| 56 | 980502 | 1.23 | 422.4 | 5.03 ± 0.11 | 5.28 ± 0.50 | W15 X1.1 | 33 | 6 | 400 | 0 | 91 |
| 57 | 980506 | 1.02 | 704.8 | 4.53 ± 0.06 | 2.45 ± 0.85 | W65 X2.7 | 48 | 13 | 600 | 0 | 127 |
| 58 | 980824 | 0.96 | 171.6 | 0.41 ± 0.01 | 9.69 ± 2.70 | E07 X1.0 | 101 | 12 | 400 | 1 | NA |
| 59 | 000714 | 0.06 | 291.3 | 3.97 ± 0.01 | 1.08 ± 0.08 | W07 X5.7 | 68 | 11 | 500 | 2 | 165 |
| 60 | 010415 | 0.92 | 115.3 | 2.55 ± 0.02 | 5.82 ± 0.31 | W85 X14 | 21 | 5 | 400 | 3 | 176 |
| 61 | 010418 | 0.51 | 159.3 | 1.55 ± 0.02 | 4.25 ± 0.44 | W120 C2.2 | NA | NA | 400 | 3 | 133 |
| 62 | 011104 | NA | NA | 1.80 ± 0.01 | 0.29 ±0.11 | W18 X1.0 | 146 | 12 | 530 | 0 | 183 |
| 63 | 011226 | NA | NA | 1.49 ±0.01 | 4.98 ± 0.21 | W54 M7 | 306 | 60 | 1000 | 1 | 123 |
| 64 | 020824 | NA | NA | 1.17 ± 0.01 | 6.13 ± 0.56 | W81 X3.1 | 83 | 14 | 1500 | 2 | 174 |
| 65 | 031028 | NA | NA | 4.36 ± 0.01 | 0.11 ± 0.09 | E08 X17 | 65 | 8 | 2100 | 4 | 122 |
| 66 | 031029 | 0.24 | 209.7 | 2.50 ± 0.01 | 0.94 ± 0.10 | W02 X10 | 41 | 8 | 2230 | 4 | 83 |
| 67 | 031102 | 0.30 | 564.3 | 1.10 ± 0.00 | 0.96 ± 0.15 | W56 X8 | 54 | 11 | 2290 | 4 | 158 |
| 68 | 050117 | NA | NA | 1.06 ± 0.02 | 1.16 ±0.10 | W25 X3.8 | 142 | 60 | 1450 | 1 | 114 |
| 69 | 050120 | 0.50 | 66.8 | 1.05 ± 0.01 | 0.51 ± 0.10 | W61 X7.1 | 93 | 16 | 1430 | 1 | NA |
| 70 | 061213 | NA | NA | 2.82 ± 0.03 | 5.60 ± 0.04 | W24 X3.4 | 81 | 16 | 690 | 0 | 145 |

[a]e/p low: (e > 1 MeV)/(p > 30 MeV)

[b]e/p high: (e > 1 MeV)/(p > 430 MeV)

[c]Fe/O low: Fe/O at 3.2–5 MeV/nuc from Wind/EPACT,normalized to average SEP value of 0.134

[d]Fe/O high: Fe/O at 50–75 MeV/nuc from ACE SIS, normalized to average SEP value of 0.134

[e]Duration above 10% of SXR peak in minutes; rise times from 10% of SXR peak to peak time in minutes

[f]Approximate areas of AR sunspots in millionths of a solar hemisphere

[g]Widths in degrees. CMEs for GLEs #33–42 from Solwind and SMM catalogs; CMEs for GLEs # 55–70 from Lasco SEEDS catalog

#33 (the background was dominated by a previous SEP event), #40 (no Fe ions detected; value is an upper limit corresponding to one Fe ion), and #50, 51 (data gaps). For GLEs # 55–70 we used fluences at 3.2–5 MeV/nuc from the EPACT instrument on the Wind spacecraft. We refer to both these data sets as Fe/O low ratios and list them in column 5 of Tables 1 and 2. For high-energy Fe/O ratios (hereafter Fe/O high) we used the published 47–80 MeV/nuc ratios (Table 2 of Tylka et al. 2005, with additional values specifically for this energy range for events #36 and #42–45) for GLEs #27–53 from the CRNE experiment on IMP-8 and 50–75 MeV/nuc ratios from the Solar Isotope Spectrometer (SIS) instrument on the ACE spacecraft for GLEs #55–70. Those ratios are given in column 6 of Tables 1 and 2. All Fe/O ratios are normalized to the average gradual SEP value of 0.134 (Reames 1998).

Since our analysis combines Fe/O measurements from four instruments on three satellites, it is important to consider the potential effect of systematic uncertainties on our correlation fits. By comparing simultaneous event-integrated Fe/O values from different instruments at nearly commensurate energy bins, we estimate the systematic uncertainties in the Fe/O values to be on the order of 5–10%. These differences are smaller than those generally found in comparing intensities and fluences; but this is not unexpected, since many of the factors contributing to instrument-to-instrument differences in intensities and fluences,

such as imperfect knowledge of geometry factors and live-time corrections, largely cancel out when taking ratios of fluences. In the correlation analyses below, we have added 5% systematic uncertainty in quadrature with the Fe/O statistical errors given in Tables 1 and 2. Doubling the systematic uncertainty to 10% causes only minor changes in the values of the correlation coefficients and their corresponding probabilities and does not affect any of our conclusions.

A measure of the importance of using two energy ranges rather than one for the e/p and Fe/O ratios is the correlation between the low and high energy parameters for each ratio. A high correlation implies significant redundancy, but a low correlation implies that the two energy ranges provide relatively independent tests for flare versus shock SEP contributions to the GLEs. For the log e/p high versus log e/p low ratios we get a correlation coefficient of $r = 0.45$ for 32 GLEs, corresponding to a random correlation probability of $P = 0.01$. A more direct comparison of logs of the >430 MeV and >30 MeV fluences, including GLEs for which we do not have the >1 MeV electron fluences, yields $r = 0.58$ for 42 GLEs. The Fe/O ratios can have strong energy dependence (Tylka et al. 2005), and we find a smaller correlation coefficient $r = 0.31$ and a random correlation probability $P = 5.2\%$ for 40 Fe/O low and high values of Tables 1 and 2. These results show a greater independence for the pair of Fe/O ratios than for the e/p ratios. Of course, this is not surprising, given that both e/p ratios use the same numerator.

We note that the range of values of each of the four particle abundance ratios of Tables 1 and 2 extends up to two orders of magnitude. It is not clear whether the correlations are better done with linear or logarithmic values of those ratios, so the correlations of the particle abundance ratios with the flare, AR, and CME parameters were done with both the linear and logarithmic values of the abundance ratios. Because some of the fluence ratios have significant uncertainties, all of our correlations coefficients have been calculated as weighted correlations, with the error bars on the e/p and Fe/O ratios taken into account. Table 3 contains the probabilities of no significant correlation, $P$, along with the correlation coefficients and number of available sample GLEs for each of these comparisons for only the weighted logarithmic abundance ratios. However, we consider as significant only those cases where $P$ is <0.01 for both the weighted logarithmic and linear values.

## 2.2 Flare Diagnostic Parameters

### *2.2.1 Flare SXR Time Scales*

The solar longitudes and peak GOES 1–8 Å SXR fluxes of the flares associated with the GLEs are given in column 7 of Tables 1 and 2 with the usual GOES CMX scales for the SXR fluxes. For each GLE we examined the associated SXR flare time profile to determine the flare duration for which the SXR flux was above the level of 10% of the peak flux, the criterion used in previous studies (CMvR; Kahler et al. 1991; Cliver 2009b). For GLE #26 we used Solrad 9 SXR data provided by the NSSDC, and for all other GLEs GOES SXR flux profiles were inspected to determine both the durations and the rise times from 10% of peak to the time of peak flux. Those flare times in minutes are given in columns 8 and 9 of Tables 1 and 2. In GLEs #29, 39, 50, and 61 the associated SXR flare was occulted behind the west limb and in GLEs #33 and 35 the peak SXR flux ≤ M1 (Cliver 2006), too small for a determination of the durations and rise times. The focus here is on the short-duration (<60 minutes) flares. Through 1990 Kahler et al. (1991) had reported 6, and we now have 13 short-duration flares among the 45 GLEs observed since 1973.

Before doing the comparison of GLE abundance ratios with the SXR times, we first test whether those times are independent of solar source longitude. If the short-duration SXR

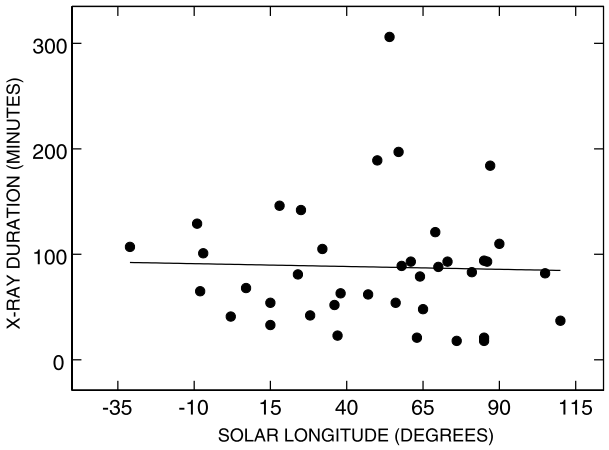


**Fig. 1** Plot of SXR flare durations in minutes versus the associated solar flare source longitudes for the GLEs of Tables 1 and 2. The line gives the least-squares best fit, but there is no significant correlation between the flare durations and solar source longitudes

flares were indeed indicative of a direct flare contribution in their associated GLEs, we would expect the short-duration events to lie predominately at well-connected (∼W 40°–W 80°) longitudes. No such predominance is seen; to the contrary, as shown in Fig. 1, 10 of 26 (38%) long-duration GLE-associated SXR flares and only 4 of 13 (31%) short-duration flares are well connected. There is thus no bias for GLEs with more short-duration flares to be well connected, and any correlation of GLE characteristics with flare timescales will be independent of magnetic connectivity.

The correlations of the e/p low, e/p high, Fe/O low, and Fe/O high parameters against the flare durations and rise times are presented in the first two rows of Table 3. For the e/p comparisons only the case of e/p low versus logs of flare rise times, shown in Fig. 2, produced a significant inverse correlation ($P = 0.004$ for 30 events). If flare timescales do order the e/p ratios, the expected trend (CMvR) would be declining e/p ratios with increasing timescales as we find in Fig. 2, but this anti-correlation is weak for the flare durations and there is no evidence for a flare timescale effect in the e/p high ratios.

In all four cases of the Fe/O comparisons we found weak trends for Fe/O to decline with increasing logs of flare timescales, as Reames et al. (1990) found earlier for Fe/C at 2–3 MeV/nuc versus H$\alpha$ flare durations and Cliver (2009b) found for a comparison of Fe/O values at 30–40 MeV/nuc versus SXR flare durations in 39 large SEP events, of which 15 were GLEs. The Fe/O low ratio is anti-correlated with the SXR duration only for log values. Since $P = 0.07$ for the linear values, that correlation is not considered significant. Our correlation coefficient of Fe/O high with flare duration was $r = -0.20$, lower than the Cliver (2009b) value of $-0.46$, and not significant at $P = 0.25$. We note that with unweighted Fe/O high values $r$ increases to $-0.28$ and $P$ decreases to 0.09, explaining some of the difference with the Cliver (2009b) result. We conclude that there is no significant correlation of Fe/O with flare SXR timescales for GLEs.

### *2.2.2 Flare Thermal SXR Fluxes and Impulsive 9 GHz Flux Densities*

Peak SXR flare fluxes are often compared with associated SEP event properties (e.g., Gopalswamy et al. 2003) to look for a role for flares in SEP production, and we have matched the abundance ratios with the logs of the GOES SXR flare peak fluxes given in column 7 of Tables 1 and 2. As indicated in the third line of Table 3, none of those ratios was significantly correlated with the logs of the SXR flare peaks. Weak trends for lower abundance ratios to

**Table 3** Probabilities of No Correlation p for GLE e/p and Fe/O Fluence Ratios with SXR Flares, ARs, CMEs, and SEP fluences

| Solar/GLE property | e/p low[a] | e/p high[b] | Fe/O low[c] | Fe/O high[d] |
|---|---|---|---|---|
| SXR Flare Duration (Log) | 0.07 (−0.33 30) | 0.37 (−0.17 29) | 1.2E−3 (−0.52 36) | 0.25 (−0.20 36) |
| SXR Flare Rise (Log) | *0.004 (−0.51 30)* | 0.08 (−0.27 29) | 0.011 (−0.42 36) | 0.41 (−0.14 36) |
| SXR Flare Peak (Log) | 0.03 (−0.38 31) | 0.03 (−0.39 30) | 0.48 (0.12 38) | 0.07 (−0.30 38) |
| ∼9 GHz Peak (Log) | 0.40 (−0.16 32) | 0.35 (−0.17 31) | 0.79 (−0.04 39) | 0.03 (−0.34 40) |
| AR Sunspot Area | 0.07 (−0.31 33) | 0.77 (−0.05 32) | 0.54 (−0.10 40) | 5.2E–4 (−0.52 41) |
| AR Nearby Regions | 0.012 (−0.43 33) | 0.07 (−0.32 32) | 0.59 (−0.09 40) | 0.31 (−0.34 41) |
| Lasco CME widths | 0.47 (−0.30 8) | 0.61 (−0.21 8) | 0.29 (−0.31 14) | 0.78 (0.08 14) |
| Solwind/SMM CME widths | 0.91 (0.04 9) | 0.53 (0.26 8) | 0.59 (−0.19 10) | 0.99 (0.004 10) |
| Longitudinal Separation | 0.58 (0.10 33) | 0.50 (−0.12 32) | 0.25 (−0.19 40) | 0.54 (−0.10 41) |
| Bckgrnd p ($E > 1$ MeV) | 0.05 (−0.36 29) | 0.27 (−0.21 29) | 0.93 (−0.02 36) | 0.05 (−0.32 37) |
| Bckgrnd p ($E > 10$ MeV) | 0.08 (−0.34 28) | 0.09 (−0.33 28) | 0.48 (−0.12 35) | 0.04 (−0.35 36) |
| Fluence e ($E > 1$ MeV) | —— | —— | 0.57 (0.10 32) | 0.012 (−0.44 32) |
| Fluence p ($E > 30$ MeV) | —— | —— | 0.03 (0.16 40) | *<1.0E–7 (−0.72 41)* |
| Fluence p ($E > 430$ MeV) | —— | —— | 0.80 (0.04 39) | 0.17 (−0.22 40) |

[a]logarithms of e/p low: (e > 1 MeV)/(p > 30 MeV)

[b]logarithms of e/p high: (e > 1 MeV)/(p > 430 MeV)

[c]logarithms of Fe/O low: (3.2–5 MeV/nuc or 4–6 MeV/nuc)

[d]logarithms of Fe/O high: (47–80 MeV/nuc or 50–75 MeV/nuc)

Values given are the probabilities $P$ that no correlations exist between the pairs of solar/SEP properties versus GLE SEP ratios. The correlation coefficient and number of sample GLEs is given in parentheses for each case. Negative correlation coefficients indicate anti-correlations, and significant correlations are italicized

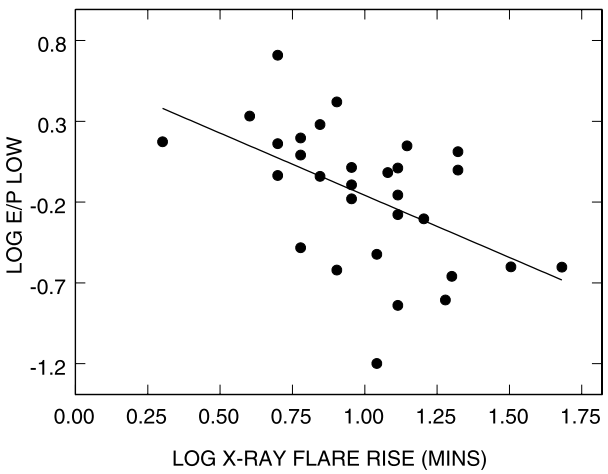


**Fig. 2** Log-log plot of the e/p low ratios versus the SXR flare rise times in minutes. The diagonal line is the least-squares best fit to the data. This is our only case of a statistically significant ($P = 0.004$) e/p correlation with SXR flare timescales

be associated with larger flares were present in both e/p and Fe/O high ratios but not in the Fe/O low ratios.

The GOES SXR peak fluxes characterize the thermal flare plasmas, but we also want a signature of the flare impulsive phase as a more direct measure of flare particle acceleration.

For this we use the peak ∼9 GHz radio bursts given for GLEs #33–69 by Cliver (2006) supplemented by the unpublished values for GLEs #26–28 and #30–32 used by Cliver et al. (1983) and a value of 6900 solar flux units for GLE #70 from Solar-Geophysical Data Reports. Correlations of the particle abundance ratios with the logs of the ∼9 GHz fluxes are given in the fourth line of Table 3. The weak trends are similar to the results for the SXR correlations.

### 2.3 Active Region Diagnostic Parameters

The active regions (ARs) associated with the fast CMEs required to produce large and energetic SEP events are generally characterized by large areas, high magnetic fluxes, strong magnetic fields, and a high degree of complexity (Wang and Zhang 2008). If the flare impulsive phase plays a significant role in the production of some GLEs, we anticipate that the associated AR might be relatively compact and isolated, possibly less likely to give rise to the large and fast CMEs usually seen in association with the most energetic SEP events. For this study we selected two crude parameters of AR size or complexity. The first is the associated AR sunspot area, reported in Solar-Geophysical Data for each day of observations by several observatories. There is considerable variance in those reported areas, both from day to day, as well as from different observatories and usually with decreasing values toward the solar limbs. From those reports of the flare AR associated with each GLE we estimated sunspot area, usually the day of or preceding the time of the GLE and listed those values in column 8 of Tables 1 and 2. Cliver (2006) found a broad range of values for sunspots associated with GLEs #33-69. We have added more GLEs to his list and made estimates for associated AR sunspots behind the limb.

As a second parameter we estimated the number of other ARs within ∼30° of the flaring active region. Again, the goal is only to get a crude measure of the coronal complexity or spatial extent involved in the development of the CME and to look for any tendency for the SEP abundance ratios to decline with increasing AR complexity or more nearby regions. We counted only the ARs with assigned NOAA numbers and found from none to four nearby ARs for each of the flare ARs, given in column 9 of Tables 1 and 2. Although these sunspot areas and nearby ARs are crude and subjective measures of the solar source regions of the GLEs, they have the advantage of good statistics in that we have those parameters for all 45 GLEs of this study.

The probabilities of no correlation with the AR parameters are given in rows 5 and 6 of Table 3. All eight ratios trend lower with larger sunspot areas and more nearby ARs. The most significant AR correlation ($P = 5.2 \times 10^{-4}$) of Table 3 is that of the Fe/O high ratio with sunspot area, shown in Fig. 3, but for the corresponding linear values $P = 0.05$. The anti-correlation trends in all these cases are consistent with more compact solar sources for GLEs with enhanced e/p and Fe/O ratios.

### 2.4 CME Diagnostic Parameters

All GLEs are associated with CMEs, so when coronagraph CME observations were available, we have compared the properties of GLEs with those of CMEs. The CME data were obtained from on-line catalogs of CMEs observed by the P78/Solwind, Solar Maximum Mission CP, and SOHO LASCO C2 and C3 coronagraphs (Boursier et al. 2009). The catalogs were compiled by human inspection of the coronagraph images, and in the case of LASCO there are additional on-line catalogs with computer-generated CME databases. One is the CACTus CME catalog (Robbrecht et al. 2009), which uses the Hough transform technique

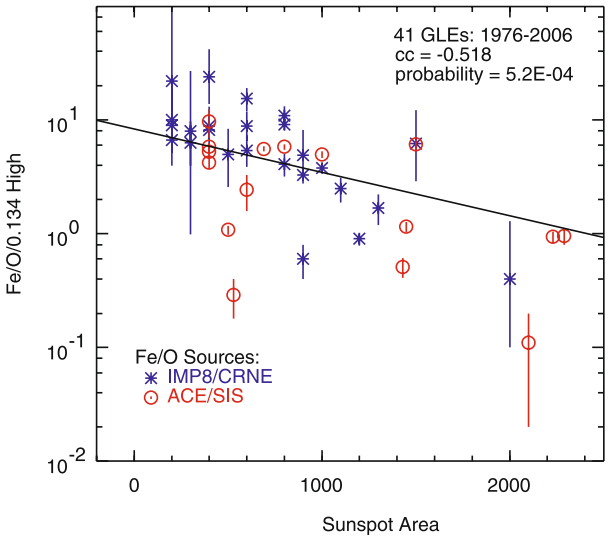


**Fig. 3** Correlation plot of the logs of Fe/O high values versus the AR sunspot areas in units of a solar hemisphere. The Fe/O values combine 25 Fe/O ratios at 47–80 MeV/nuc (IMP-8/CRNE) and 16 Fe/O at 50–75 MeV/nuc (ACE/SIS) ratios. The diagonal line is the least squares best fit to the data

to detect motion of the brightest structures of CMEs. The more recent SEEDS (Olmedo et al. 2008) and ARTEMIS (Boursier et al. 2009) catalogs are based on automated detection of CMEs in the LASCO C2 coronagraph observed at ∼2–6 $R_{\odot}$.

The CMEs associated with large SEP events are usually fast ($v > 900$ km/s) and wide ($W > 60°$) (Gopalswamy et al. 2008) and those with GLEs are much faster on average than those associated with other SEP events (Gopalswamy et al. 2005a). Our interest here is to examine the CME angular widths $W$ as possible proxies of either the timescales of the associated flares or of the sizes of the regions in which SEPs may be produced. A comparison of the LASCO fast ($v > 1000$ km/s) CMEs between the CDAW (human-generated) and CACTus catalogs shows that the CDAW CME widths are considerably wider (Yashiro et al. 2008), but for the GLEs nearly all associated CMEs are halos ($W > 180°$, and mostly 360°) in both catalogs. Another comparison of CME properties of all four LASCO catalogs shows best agreement between the ARTEMIS and SEEDS catalogs (Boursier et al. 2009), which better reflect the early phases of LASCO C2 observations. A recent analysis of LASCO CMEs based on a multiscale method convolving high and low-pass filters with CME images has shown (Byrne et al. 2009) that multiscale values agree much better with the generally smaller SEEDS CME widths than with the larger CACTus and CDAW values. Of the 13 SEEDS GLE-associated CMEs the widths $W$ agreed to within 30° with those of ARTEMIS except for 4 cases. For GLEs #59 and 62 no ARTEMIS CME is given; for #56 the SEEDS lists separate east and west limb CMEs and ARTEMIS a single broad CME; and for #63 the broader ARTEMIS width applies to a later stage of the CME than does the narrower SEEDS width. Although clearly subject to projection effects (Vršnak et al. 2007), we have therefore used the GLE CME width of SEEDS to compare with SEP abundance parameters. There are 16 GLEs during the LASCO era, but not all have measured CME widths.

The few Solwind and SMM CME widths from the earlier period, derived from human inspection and not readily compared to the computer-generated LASCO widths, are listed in the last column of Table 1. Within the limited statistics of the earlier 11 Solwind or SMM and the later 14 SEEDS CME widths we again find in rows seven and eight of Table 3 no significant correlations of Fe/O or e/p ratios with $W$.

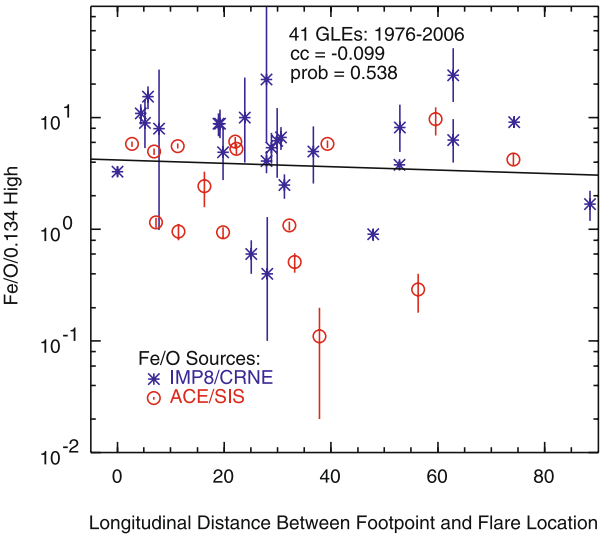


**Fig. 4** Correlation plot of the logs of Fe/O high values versus the solar longitudinal separations between the source regions and solar footpoints, which show no significant correlation. The Fe/O values combine 25 Fe/O ratios at 47–80 MeV/nuc (IMP-8/CRNE) and 16 Fe/O at 50–75 MeV/nuc (ACE/SIS) ratios. The *diagonal line* is the weighted least-squares best fit to the data

## 2.5 Solar Longitudinal Distributions of Abundance Ratios

Evidence for flare effects in GLEs may also be found by comparing the abundance ratios with the solar source longitudes of the associated flares. Enhanced e/p (CMvR; Cliver and Ling 2007) and Fe/C (Cane et al. 1991) and Fe/O (Cane et al. 2006) ratios in SEP events have been associated with well connected solar longitudes. However, Tylka et al. (2005) cautioned that enhanced Fe/O above ∼10 MeV/nucleon can also be found in far-eastern events, such as the 1999 January 20 event, for which Cane et al. (2002) put the source region at E95°. Cliver and Ling (2007) found almost no difference in e/p ratios in a comparison of magnetically well connected (W20°–W90°) and poorly connected large SEP events.

We have compared the SEP abundance ratios with the absolute values of the displacement longitudes of their source regions from the magnetic connection footpoints. We averaged 1-hr solar wind speeds for the first 6 hours of each GLE beginning with the baseline start times recommended at the Bartol web site at http://neutronm.bartol.udel.edu/~pyle/GLE_List.txt. The average and the standard deviation of the six speeds were used to calculate the connection longitude assuming a rotation rate of 13.2°/day. The corresponding standard deviations of the calculated longitudes are typically 1° to 2°, probably less than the uncertainty in assigning flare longitudes. We assumed a nominal 400 km/s for the 13 GLEs, #37–42, 44, 45, 48–51, and 54, for which solar wind speeds were not available. The results given in the ninth line of Table 3 show no significant correlations with solar source longitudes for the e/p ratios and for the Fe/O high abundance ratio shown in Fig. 4. We conclude that the longitude distributions of the SEP abundance ratios provide no evidence of flare effects in GLEs.

## 2.6 SEP Event Background Intensities

An important factor contributing to high SEP event intensities is enhanced preceding interplanetary SEP backgrounds (Kahler 2001; Cliver 2006). If CME-driven shocks are accelerating ambient coronal/interplanetary particles, then the abundances of seed particles of preceding SEP events could be an important factor for the SEP elemental ratios. Conversely,

if flare sources are dominant in GLE SEPs, then no abundance correlations with SEP backgrounds are expected. We have compared the e/p and Fe/O ratios of Table 2 with the logs of the background IMP8 or GOES $E > 1$ MeV and $E > 10$ MeV proton intensities measured on days preceding the GLEs. This provided a sample of 35 to 37 Fe/O ratios and 28 to 29 e/p ratios, but in all eight cases $P > 0.04$ (Table 3), so the background correlations were not significant. GLEs are often members of sequences of large SEP events, but we find no significant correlations of the Fe/O or e/p abundance ratios with the log intensities of the preceding SEP backgrounds. However, with increasing background intensities all the e/p and Fe/O ratios trended to lower values.

### 2.7 SEP Event Fluence Diagnostics

To search our data sets for further clues to the relationship between flare and shock contributions to the GLE ion compositions we compared the event Fe/O abundance ratios with the GLE fluences of $E > 1$ MeV electrons and $E > 30$ MeV and $E > 430$ MeV protons, which were separately calculated to determine the e/p low and high ratios of Tables 1 and 2. Those correlations are shown in the last three rows of Table 3. The only significant (both log and linear) Fe/O high correlation is the anti-correlation with the $E > 30$ MeV fluences shown in Fig. 5. Tylka et al. (2005) also reported an anti-correlation of $r = -0.40$ based on a sample of large events of Cycle 23 at lower (30 to 40 MeV/nuc) energies. The Fe/O high ratios also show negative but not significant anti-correlations with the $E > 1$ MeV electron and $E > 430$ MeV proton fluences. In all cases the Fe/O high ratios decline toward normalized coronal values of unity with increasing electron or proton event fluences. Although the three Fe/O low correlations are not significant, their correlation coefficients are positive, contrary to those of Fe/O high. We note that Reames and Ng (2010) have studied streaming-limited intensities in GLEs and find a spectral flattening and convergence of the Fe and O spectra toward lower ($\leq 5$ MeV/nuc) energies. The result of the streaming limit is to cause Fe/O to rise in the energy range we defined for Fe/O low. To determine the effect of the largest fluence GLEs, which are heavily weighted statistically, on the Fe/O low fluence correlations, we selected the fluence case with the most significant ($P = 0.03$) positive correlation, that

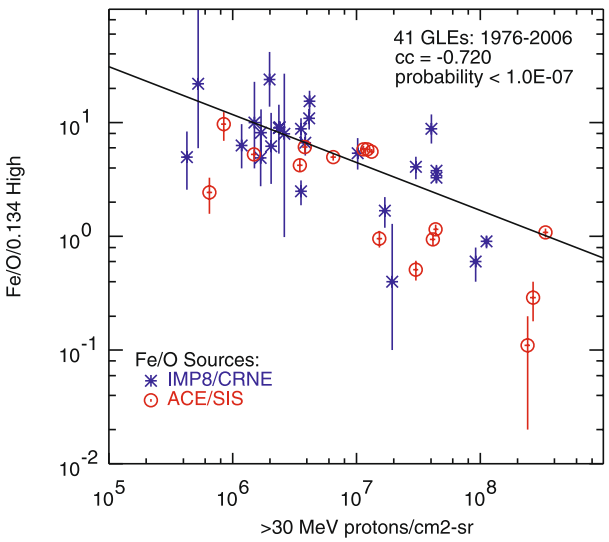


**Fig. 5** Logs of Fe/O high values versus the $E > 30$ MeV proton fluences. The *diagonal line* is the least-squares best fit to the data

of $E > 30$ Mev p. The log correlation recalculated without the three largest fluence GLEs (#59, 62, and 65) yielded an r changed from 0.16 for all 40 GLEs to $-0.13$ for 37 GLEs. Thus we conclude that except for the distorting effects of streaming limits both the Fe/O low and high fluence correlations are likely negative.

## 3 Discussion

The question of how acceleration of SEPs is effected in a combined solar eruptive flare and CME-shock scenario is a continuing challenge to our understanding of SEP events. The occurrence of low-energy ($E < 10$ MeV/nuc) $^3$He-rich events associated with small impulsive flares and the large high-energy ($E > 10$ MeV/nuc) SEP events following shocks driven by fast and wide CMEs has made clear that both processes play important roles (Klecker et al. 2007). In typical large solar events with both flares and fast and wide CMEs the question is to determine the flare and shock acceleration processes and contributions to the subsequent SEP events as functions of particle species, event intensity/fluence, and energy range. That question becomes more sharply defined when we turn to GLEs and ask whether flare effects can be ascertained in the highest observed SEP energy ranges. The relatively short timescales of $\sim$ GeV proton and $\sim$ MeV electron intensities has encouraged investigators to look for separate flare and shock phases or components in the rise phases of GLEs. As reviewed in Sect. 1.2, there is disagreement about the existence of two components in the GLE rise phases, and even if we agree on one component, whether that component is produced in a flare or a CME-driven shock scenario.

The goal of this work has been to extract from a statistical analysis of the limited data set of SEP abundance ratios and fluences of the last 45 GLEs any indications of a significant role of flares in producing some observable effect on the SEP composition. That role may consist of either a direct and independent injection of flare SEPs into the interplanetary medium along with the shock-accelerated SEPs or a production of flare suprathermal or low-energy seed particles for the shock. The approach here is to examine the extent to which any of the various flare, CME, or AR parameters organize the variability in SEP e/p and Fe/O abundance ratios, all of which range over more than an order of magnitude in this sample of GLEs. One caveat is that here we have not considered the role of energy spectral variations (Tylka et al. 2005) in the calculated ratios.

Our primary aim was to look at flare SXR timescale parameters since that is where some earlier suggestive results (CMvR; Reames et al. 1990; Cliver 2009b) were found. We extended the survey to include some source AR characteristics which might give clues to the importance of AR magnetic complexity or CME source structures that can also be important in determining GLE abundance ratios. We have focused on the probability of an apparent correlation arising randomly from uncorrelated parameters ($P$ in Table 3) rather than on the correlation coefficients because the basic question is not how well any pair of SEP and flare parameters are correlated, but rather whether a given parametric correlation is significant. From the various correlations we considered only those with the lowest ($P < 0.01$) probability of random associations for both log and linear values of the weighted abundance ratios while recognizing that general trends of the correlations, even when not significant, may also provide some guidance. We considered as flare signatures relatively high e/p and Fe/O ratios, following the earliest work of CMvR, Reames (1990) and Reames et al. (1990).

The principal result of the abundance correlations with the flare SXR timescales is a significant result in only one case, the anti-correlation of e/p low versus the flare rise time, but we find the general trends found in earlier works (Nitta et al. 2003a;

Cliver 2009b) that the e/p and Fe/O ratios decrease with increasing flare timescales. This might be taken as evidence of a role for flare particles in GLEs, but we suggest that it more likely results from an association of a CME characteristic, such as width $W$, with the flare timescale. A correlation of CME width with flare duration was found in the Solwind CME data set (Kahler et al. 1989), and Yashiro and Gopalswamy (2009) found correlations of both CME speeds and widths with SXR flare durations. A recent comparison (Yashiro, private communication) of LASCO CME widths and durations of associated M1–M3 flares at central meridian distances of $>60°$ yielded correlation coefficients of $r \sim 0.6$ on log-log plots. Recently, flare timescales have also been correlated with positive post-impulsive phase accelerations of CMEs (Cheng et al. 2010) and to longer poloidal flux injections in CMEs (Chen and Kunkel 2010), either of which might lead to faster or more energetic CMEs capable of shock acceleration to GeV energies.

A further diagnostic test for flare contributions to GLEs is whether the GLEs with enhanced e/p and Fe/O ratios are magnetically well connected, and *we found no significant correlations of any ratio with longitudinal separations of the source regions from the magnetic connection footpoints* (Table 3). This result agrees with the finding of Cliver and Ling (2007) that their e/p ratios ($E > 0.5$ MeV e and $E > 10$ and 30 MeV p) of 110 SEP events were independent of longitude. Lack of good magnetic connection is another indication that the flare parameters are proxies for a CME characteristic related to shock acceleration rather than signatures of flare acceleration processes.

The search for abundance correlations with solar source spatial sizes or magnetic complexity was based on the relatively crude parameters of AR sunspot area and number of neighboring ARs. There was an anti-correlation of the Fe/O high logs (but not linear values) with those parameters (Fig. 3), but in all cases the general trends were for lower e/p and Fe/O ratios with increasing AR sunspot areas and numbers of AR neighbors. If this suggests a significant role for flares, then flare effects in GLEs will be most observable in the smaller or more confined flare regions. This is somewhat contrary to the finding of Nitta et al. (2003b) of a tendency for simple or weak sunspot groups tend to be associated only with large SEP events with gradual SEP characteristics, but their event sample was small. We also must consider that our trends may tell us more about the associated CME properties than about the associated flares although Gopalswamy et al. (2005b) found little correlation between either peak SEP event intensities or CME speeds with AR areas. We also attempted to look for correlations of GLE abundance ratios directly with measured CME widths, but this was generally unsuccessful because of (1) the small numbers of observed associated CMEs, (2) the different techniques of measuring the earlier Solwind/SMM and the later LASCO SEEDS widths, and (3) the inherent difficulty of projection effects, particularly for large CMEs. However, as with the sunspot areas and numbers of neighboring ARs, we found weak trends for lower abundance ratios with larger CME widths. Thus the abundance correlations with indices of spatial source size indicate that larger sizes favor lower SEP abundance ratios.

The flare peak ~9 GHz flux densities are taken as signatures of flare impulsive phase acceleration, so a significant correlation of SEP abundance ratios with that parameter might be the best evidence for a flare role in GLEs. The ratios decline toward coronal values with increasing burst flux densities, *exactly the opposite of what we might expect from a significant flare role*, but the correlations are not significant. Except for the Fe/O low ratio, the abundance correlations with the flare SXR peak fluxes also produced a similar result. The general trends were again for slight declines of the e/p and Fe/O ratios with increasing flare peak fluxes, but with considerable scatter of the data. Thus we find that flare intensities reflecting either thermal flare plasmas or impulsive particle acceleration do not provide an

ordering to the GLE abundance ratios. This we take as evidence against significant flare production of either directly injected energetic particles or production of suprathermal seed particles.

The inverse correlations between the Fe/O ratios and the SEP fluences could alternatively provide an argument for a role for flare particles in which the contribution of flare particles is limited and increasingly diluted in the largest fluence events. In this scenario the trends for decreasing abundance ratios with increasing SXR and ∼9 GHz flux densities could be interpreted in terms of the Big Flare Syndrome (Kahler 1982) in which all eruptive event emissions tend to scale together, in this case the SEP fluences and the associated flare peak fluxes. That interpretation implies, however, that the flare SXR and ∼9 GHz flux densities are not signatures of flare SEP contributions, and it is not obvious why the *ratios* of the SEP fluences should decline with flare size. Furthermore, if flare particles are major contributors to GLEs, then we have no reason to expect the observed weak trend of lower GLE abundance ratios with increasing background SEP intensities. We prefer the alternative shock interpretation of Tylka et al. (2005) that a high Fe/O ratio is a signature of a shock that is quasi-perpendicular while near the Sun, preferentially drawing its seed population from flare remnants. Because quasi-perpendicular shocks require a higher injection energy, they generally draw from a smaller seed population than quasi-parallel shocks. As a result, events with quasi-perpendicular near-Sun shocks will generally have smaller proton fluences, at least at the higher energies produced primarily while the shock is near the Sun.

## 4 Summary

Our extensive parametric search has yielded no compelling positive result in support of a role for flares in the generation of SEPs in GLEs. We have examined the correlations of Fe/O and e/p abundance ratios, each at two different energies, versus various observables related to flares, ARs, and CMEs. We assumed that if flares play an important role in GLEs, then the enhanced abundance ratios should preferentially be associated with shorter SXR timescales, higher intensities of SXR and ∼9 GHz emissions, and small longitudinal separations from the flare site. We also examined AR characteristics, as measured by sunspot area and number of other ARs near the flare site, motivated by the assumption that larger sunspot areas and larger numbers of nearby ARs favor the magnetic complexity that produces large, fast CMEs and hence copious particle acceleration by the CME-driven shock that would tend to mask the flare contribution. Finally, we also examined correlations with CME widths and pre-event background levels, for which larger values are known to favor particle production by CME-driven shocks, again potentially leading to anti-correlations with enhanced abundance ratios. In our analysis we adopted a fairly stringent requirement for deeming a correlation to be significant, appropriate to the large number of correlations we examined. Specifically, we required that the observed correlation coefficient must have less than 1% random probability. Since it is generally unclear whether correlations should be done versus the abundance ratio or its logarithm, we further required that this threshold be met for both cases. Of the 40 correlations we examined, only one—the anti-correlation of the lower-energy e/p to e/p low ratio versus the rise time of the soft $X$-ray flare, shown in Fig. 2—was found to be significant by these standards. As detailed in Table 3, there are two other cases in which the correlation passed the 1% threshold for the logarithms of the ratios but not for the ratios themselves. Figure 3 is the better example among these two cases.

In general, the GLEs with the highest e/p and Fe/O ratios, the best candidates for contributions from flare acceleration processes, are not better magnetically connected to the

source regions (Fig. 4) and not more positively correlated with either impulsive or thermal phase flare intensities. The cases of best SEP abundance correlations suggest that the high e/p and Fe/O ratios are found in GLEs associated with spatially compact and magnetically simple source regions (Fig. 3). The fact that comparable correlations are found between the SEP abundance ratios and the SXR flare timescales (Fig. 2) may simply mean that the short flare timescales are the temporal analogue of smaller spatial size scales. The small spatial scales may also have implications for the evolution of shock geometry in an event (Tylka et al. 2005; Tylka and Lee 2006, Cliver 2009a, 2009b).

Further work to determine how flare timescales and solar source region sizes are related to CME properties such as width $W$, acceleration, kinetic energy, or speed $v$, may then provide a framework to understand the high variability of the SEP abundance ratios with source regions of small size and short flare timescales. In addition to the CME properties, there is a requirement to determine and incorporate the SEP seed particle populations into a model with CME-driven shocks as the only important acceleration mechanism. It would then complement the recent results of Reames (2009b) showing that all particle species and energies observed in GLE onsets arise from single solar release points whose heights tend to increase with longitudinal separation from the source region, as expected in shock acceleration.

**Acknowledgements** A.J.T. and W.F.D. were supported by NASA DPR NNG06EC551. A.J.T. was also supported by the Office of Naval Research, and S.W.K. and E.W.C. were funded by AFOSR task 2301RDZ4.

## References

Y. Boursier, P. Lamy, A. Llebaria, F. Goudail, S. Robelus, Sol. Phys. **257**, 125–147 (2009)
J.P. Byrne, P.T. Gallagher, R.T.J. McAteer, C.A. Young, Astron. Astrophys. **495**, 325 (2009)
H.V. Cane, D. Lario, Space Sci. Rev. **123**, 45–56 (2006)
H.V. Cane, R.E. McGuire, T.T. von Rosenvinge, Astrophys. J. **301**, 448–459 (1986)
H.V. Cane, D.V. Reames, T.T. von Rosenvinge, Astrophys. J. **373**, 675–682 (1991)
H.V. Cane, W.C. Erickson, N.P. Prestage, J. Geophys. Res. **107**, 1315 (2002)
H.V. Cane, T.T. von Rosenvinge, C.M.S. Cohen, R.A. Mewaldt, Geophys. Res. Lett. **30**, 8017 (2003)
H.V. Cane, R.A. Mewaldt, C.M.S. Cohen, T.T. von Rosenvinge, J. Geophys. Res. **111**, A06S90 (2006)
H.V. Cane, I.G. Richardson, T.T. von Rosenvinge, in *Proc. 30th ICRC*, vol. 1 (2008), pp. 67–70
J. Chen, V. Kunkel, Astrophys. J. **717**, 1105–1122 (2010)
X. Cheng, J. Zhang, M.D. Ding, W. Poomvises, Astrophys. J. **712**, 752–760 (2010)
A. Ciaravella, J.C. Raymond, J. Li, P. Reiser, L.D. Gardner, Y.-K. Ko, S. Fineschi, Astrophys. J. **575**, 1116–1130 (2002)
E.W. Cliver, Astrophys. J. **639**, 1206–1217 (2006)
E.W. Cliver, in *Universal Heliospherical Processes*, ed. by N. Gopalswamy, D.F. Webb. IAU Symp., vol. 257 (Cambridge Univ. Press, Cambridge, 2009a), pp. 401–412
E.W. Cliver, Cent. Eur. Astrophys. Bull. **33**, 253–270 (2009b)
E.W. Cliver, A.G. Ling, Astrophys. J. **658**, 1349–1356 (2007)
E.W. Cliver, A.G. Ling, Astrophys. J. **690**, 598–609 (2009)
E.W. Cliver, S.W. Kahler, H.V. Cane, M.J. Koomen, D.J. Michels, R.A. Howard, N.R. Sheeley Jr., Sol. Phys. **89**, 181–193 (1983)
E.W. Cliver, S.W. Kahler, D.V. Reames, Astrophys. J. **605**, 902–910 (2004)
M.I. Desai, G.M. Mason, R.E. Gold, S.M. Krimigis, C.M.S. Cohen, R.A. Mewaldt, J.E. Mazur, J.R. Dwyer, Space Sci. Rev. **130**, 243–253 (2007)
N. Gopalswamy, S. Yashiro, A. Lara, M.L. Kaiser, B.J. Thompson, P.T. Gallagher, R.A. Howard, Geophys. Res. Lett. **30**, 8015 (2003)
N. Gopalswamy, S. Yashiro, S. Krucker, G. Stenborg, R.A. Howard, J. Geophys. Res. **109**, A12105 (2004)
N. Gopalswamy, H. Xie, S. Yashiro, I. Usoskin, in *Proc. 29th ICRC*, vol. 1 (2005a), pp. 169–172
N. Gopalswamy, S. Yashiro, S. Krucker, R.A. Howard, in *Coronal and Stellar Mass Ejections*, ed. by K.P. Dere, J. Wang, Y. Yan. IAU Symp., vol. 226 (Paris, IAU, 2005b),

N. Gopalswamy, S. Yashiro, S. Akiyama, P. Mäkelä, H. Xie, M.L. Kaiser, R.A. Howard, J.L. Bougeret, Ann. Geophys. **26**, 3033–3047 (2008)
S.W. Kahler, J. Geophys. Res. **87**, 3439–3448 (1982)
S.W. Kahler, J. Geophys. Res. **106**, 20947–20955 (2001)
S.W. Kahler, M.A. Shea, D.F. Smart, E.W. Cliver, in *Proc. 22nd ICRC*, vol. 3 (1991), pp. 21–24
S.W. Kahler, N.R. Sheeley Jr., M. Liggett, Astrophys. J. **344**, 1026–1033 (1989)
S.W. Kahler, D.V. Reames, N.R. Sheeley Jr., Astrophys. J. **562**, 558–565 (2001)
B. Klecker, E. Möbius, M.A. Popecki, L.M. Kistler, H. Kucharek, M. Hilchenbach, Adv. Space Res. **38**, 493–497 (2006)
B. Klecker, E. Möbius, M.A. Popecki, Space Sci. Rev. **130**, 273–282 (2007)
Y.-K. Ko, J.C. Raymond, J. Lin, G. Lawrence, J. Li, A. Fludra, Astrophys. J. **594**, 1068–1084 (2003)
L. Kocharov, J. Torsti, Sol. Phys. **207**, 149–157 (2002)
R.A. Leske, R.A. Mewaldt, C.M.S. Cohen, A.C. Cummings, E.C. Stone, M.E. Wiedenbeck, T.T. von Rosenvinge, Space Sci. Rev. **130**, 335–340 (2007)
G.M. Mason, J.E. Mazur, J.R. Dwyer, J.R. Jokipii, R.E. Gold, S.M. Krimigis, Astrophys. J. **606**, 555–564 (2004)
S. Masson, K.-L. Klein, R. Bütikofer, E. Flückiger, V. Kurt, B. Yushkov, S. Krucker, Sol. Phys. **257**, 305–322 (2009)
J.E. Mazur, G.M. Mason, M.D. Looper, R.A. Leske, R.A. Mewaldt, Geophys. Res. Lett. **26**, 173–176 (1999)
K.G. McCracken, H. Moraal, P.H. Stoker, J. Geophys. Res. **113**, A12101 (2008)
L.I. Miroshnichenko, E.V. Vashenyuk, Yu.V. Balabin, J. Perez-Peraza, B.B. Gvozdevsky, in Proc. 31st ICRC (2009, in press). http://icrc2009.uni.lodz.pl/proc/pdf/icrc1171.pdf
H. Moraal, J.P.L. Reinecke, K.G. McCracken, in Proc. 31st ICRC (2009, in press). http://icrc2009.uni.lodz.pl/proc/pdf/icrc1553.pdf
N.V. Nitta, E.W. Cliver, A.J. Tylka, Astrophys. J. **586**, L103–L106 (2003a)
N.V. Nitta, E.W. Cliver, A.J. Tylka, P. Smit, in *Proc. 28th ICRC*. vol. 6 (2003b), pp. 3363–3366
E.I. Novikova, W.F. Dietrich, A.J. Tylka, J. Collins, B.F. Phlips, Adv. Space Res. **46**, 31–43 (2010)
O. Olmedo, J. Zhang, H. Wechsler, A. Poland, K. Borne, Sol. Phys. **248**, 485–499 (2008)
J. Perez-Peraza, E.V. Vashenyuk, L.I. Miroshnichenko, Yu.V. Balabin, A. Gallegos-Cruz, Astrophys. J. **695**, 865–873 (2009)
D.V. Reames, Astrophys. J. Suppl. Ser. **73**, 235–251 (1990)
D.V. Reames, Rev. Geophys. **33**, 585–589 (1995)
D.V. Reames, Space Sci. Rev. **85**, 327–340 (1998)
D.V. Reames, Space Sci. Rev. **90**, 413–491 (1999)
D.V. Reames, Astrophys. J. **540**, L111–L114 (2000)
D.V. Reames, Astrophys. J. **571**, L63–L66 (2002)
D.V. Reames, Astrophys. J. **693**, 812–821 (2009a)
D.V. Reames, Astrophys. J. **706**, 844–850 (2009b)
D.V. Reames, C.K. Ng, Astrophys. J. **610**, 510–522 (2004)
D.V. Reames, C.K. Ng, Astrophys. J. **723**, 1286–1293 (2010)
D.V. Reames, H.V. Cane, T.T. von Rosenvinge, Astrophys. J. **357**, 259–270 (1990)
D.V. Reames, J.P. Meyer, T.T. von Rosenvinge, Astrophys. J. Suppl. Ser. **90**, 649–667 (1994)
D.V. Reames, B.R. Dennis, R.G. Stone, R.P. Lin, Astrophys. J. **327**, 998–1008 (1988)
E. Robbrecht, D. Berghmans, R.A.M. Van der Linden, Astrophys. J. **691**, 1222–1234 (2009)
A. Saiz, D. Ruffolo, M. Rujiwarodom, J.W. Bieber, J. Clem, P. Evenson, R. Pyle, M.L. Duldig, J.E. Humble, in *Proc. 29 ICRC* (2005), p. 229
A.J. Tylka, M.A. Lee, Astrophys. J. **646**, 1319–1334 (2006)
A.J. Tylka, W.F. Dietrich, in Proc. 31st ICRC (2009, in press). http://icrc2009.uni.lodz.pl/proc/pdf/icrc0273.pdf
A.J. Tylka, C.M.S. Cohen, W.F. Dietrich, M.A. Lee, C.G. Maclennan, R.A. Mewaldt, C.K. Ng, D.V. Reames, Astrophys. J. **625**, 474–495 (2005)
A.J. Tylka, C.M.S. Cohen, W.F. Dietrich, M.A. Lee, C.G. Maclennan, R.A. Mewaldt, C.K. Ng, D.V. Reames, Astrophys. J. Suppl. Ser. **164**, 536–551 (2006)
E.V. Vashenyuk, Yu.V. Balabin, B.B. Gvozdevsky, in Proc. 31st ICRC (2009, in press). http://icrc2009.uni.lodz.pl/proc/pdf/icrc1304.pdf
B. Vršnak, D. Sudar, D. Ruždjak, T. Žic, Astron. Astrophys. **469**, 339–346 (2007)
Y. Wang, J. Zhang, Astrophys. J. **680**, l516–l522 (2008)
S. Yashiro, N. Gopalswamy, in *Universal Heliospherical Processes*, ed. by N. Gopalswamy, D.F. Webb. IAU Symp., vol. 257 (Cambridge Univ. Press, Cambridge, 2009), pp. 233–242
S. Yashiro, N. Gopalswamy, E.W. Cliver, D.V. Reames, M.L. Kaiser, R.A. Howard, in *The Solar-B Mission and the Forefront of Solar Physics*, ed. by T. Sakurai, T. Sekii. Conf. Ser., vol. 325 (ASP, San Francisco, 2004), pp. 401–408
S. Yashiro, G. Michalek, N. Gopalswamy, Ann. Geophys. **26**, 3103–3112 (2008)